

Wind energy potential assessment in Naxos Island, Greece

Ioannis Fyrippis, Petros J. Axaopoulos*, Gregoris Panayiotou

Energy Technology Department, Technological Educational Institute of Athens, Agiou Spyridona Street, 12210 Egaleo, Athens, Greece

ARTICLE INFO

Article history:

Received 16 February 2009
Received in revised form 19 May 2009
Accepted 21 May 2009
Available online 18 June 2009

Keywords:

Wind potential
Wind speed
Wind power density
Weibull–Rayleigh distribution
Aegean Sea
Greece

ABSTRACT

The current paper presents an investigation of the wind power potential of Koronos village, a remote location in the northeastern part of Naxos Island, Greece, using real wind data by a measurement mast. The obtained wind characteristics were statistically analysed using the Weibull and Rayleigh distribution functions. The results from this investigation showed that the selected site falls under Class 7 of the international system of wind classification as the mean annual wind speed recorded in the area was 7.4 m/s and the corresponding annual mean power density was estimated to be 420 W/m². Furthermore, the prevailing wind directions characterising the area were the northeastern and the north–northeastern. From the statistical analysis of these results, it was revealed that the Weibull model fitted the actual data better. This remark was further enhanced by the evaluation of the performance of these two distributions.

© 2009 Elsevier Ltd. All rights reserved.

1. Introduction

The world energy consumption has increased significantly in the last decades and this growth seems to continue with fossil fuels providing the majority of this energy. However, the use of fossil fuels creates serious environmental problems, including acid emissions, air pollution and finally the climate changes. Many countries worldwide recognise that current energy trends are not sustainable and that a better balance must be found between energy security, economic development, and protection of the environment.

Here comes the significance of sustainable energy sources like wind. Wind power has a remarkably rapid growth in the past twenty years, and now is a mature, reliable and efficient technology for electricity production.

Even though the use of wind energy been studied for many years due to the need for ‘greener’ ways of generating electricity, there has only been very broad information on the wind potential in the Aegean Sea and especially in remote locations. Mariopoulos and Karapiperis [1] carried out a preliminary study on the use of wind energy in Greece. Their work was expanded by Galanis [2] and Tselepidaki et al. [3]. Later, in 1983, Lalas et al. [4] used data from the Hellenic National Meteorological Station for 22 locations around Greece to predict the corresponding wind potentials. The results of these works presented mainly an overview of the wind potential around Greece in general, and identified the high wind energy capacity existing over the Aegean Sea specifically. Nearly

a decade later, Katsoulis [5] analysed the updated version (42 locations instead of 22) of Lalas et al. [4] data, part of which was obtained from Naxos station. Kaldellis has performed an extensive research in the utilisation of the wind potential of the Aegean Sea [6,7]. In 2002, he used long-term (i.e. 4 years) wind speed data obtained from the Greek Public Power Corporation, for Kithnos, a relatively small island located in the southwest of the Aegean Sea in order to suggest the usage of a stand-alone wind power system for covering the energy requirements of the island [8]. The analysis of the wind data showed that the island was characterised by strong winds, which reach an annual mean value of 7 m/s at 10 m height in several locations. The windiest season proved to be the winter and the calmest was towards the end of spring and the beginning of summer. The wind potential of the northwestern part of the Aegean Sea has been extensively studied by Turkish researchers. Ozerdem and Turkeli [9], investigated the wind characteristics of Izmir, which is located near the Turkish coastline along the Aegean Sea. The results showed that the average speed at 10 m was 7.03 m/s whereas at 30 m the corresponding value was 8.14 m/s. Akpınar [10], statistically investigated the wind energy potential of the overall area of Elazığ and the nearby regions of Maden, Agin and Keban (all situated along the coastline of the Marmara Sea) using wind speed data recorded over 72 months and by applying on it Weibull and Rayleigh distributions. The results of this investigation showed that Maden is ideal for grid-connected applications since the annual mean wind power density was found to be 246.27 W/m². On the contrary, the annual mean wind power densities in Elazığ, Agin and Keban regions were not high enough for electrical production. The maximum annual mean

* Corresponding author. Tel.: +30 2105385396; fax: +30 2105385733.
E-mail address: pax@teiath.gr (P.J. Axaopoulos).

wind speed recorded was 5.66 m/s in Maden. Further research in the northwestern Marmara region in Turkey was performed [11] and it was found that the higher mean wind speeds occurred during winter, while the lower values appeared in autumn. Furthermore, they indicated that the Weibull shape parameter k ranged between 1.57 in autumn and 2.21 in summer, while the corresponding scale parameter c ranged between 4.56 m/s in autumn and 5.93 m/s in winter, respectively. Finally, the south region of Marmara Sea was covered by a study [12]. The results obtained showed that the annual mean wind speed for the period under investigation was 7.08 m/s. It was found that the average values of the Weibull parameters k and c were 1.78 and 7.97 m/s, respectively. As far as the calculated wind power was concerned, it was found that the lowest value was 335 W/m² observed during winter, while the highest was 925 W/m² and it was obtained during summer.

As a step towards assessing the wind potential of the Aegean Sea the current study was set to evaluate real wind data. The wind speed and direction as well as the availability, the duration and the diurnal variation were assessed, and the results were statistically compared with Weibull and Rayleigh distribution functions. Both distribution functions were assessed in order to determine which described the actual data better.

2. Methodology and materials

2.1. Site description

Naxos Island (latitude 37°06' N), is situated towards the middle of Cyclades, a complex of small to medium size islands, in the southern part of the Central Aegean Sea, and it is characterised by strong winds. The topography of the area is typically Aegean, characterised by hills and mountains covered with bushes, and very limited flat fields. The site location is situated at approximately 700 m from the sea level and is marked with red¹ arrow in Fig. 1. Additionally, the soil depth is quite low, making the site unsuitable for any agricultural activity, and therefore no disturbance is caused to the local eco-system.

2.2. Wind data measurement mast

A 10 m height mast, made out of steel in solid tubular form was used, strengthened by guyed wires in order to keep it in a vertical position (Fig. 2). A cup anemometer and a wind vane were both installed at the top of the mast. The temperature and the relative humidity were also measured using a thermometer and a hygrometer, respectively. Data obtained from all the installed instruments was acquired using a data logger. The data logger, which was connected with all the available sensors on the mast, recorded and stored the collected data in time – series format. Once the required data was stored, the transferring of it to the laboratory in Athens for processing was achieved via a GSM method used by the data logger. Finally, the required power for all the previously mentioned instruments was provided by 12 V battery, charged by a pv panel.

The reason for performing wind measurements at 10 m height was that according to [5,7], for climatological and practical reasons it has been agreed that this should be the standard meteorological reference level in order to achieve representative recording of the wind potential of the area. Furthermore, the wind speed at higher heights could be calculated using the power law.



Fig. 1. Map of Naxos Island showing the wind data measurement mast.

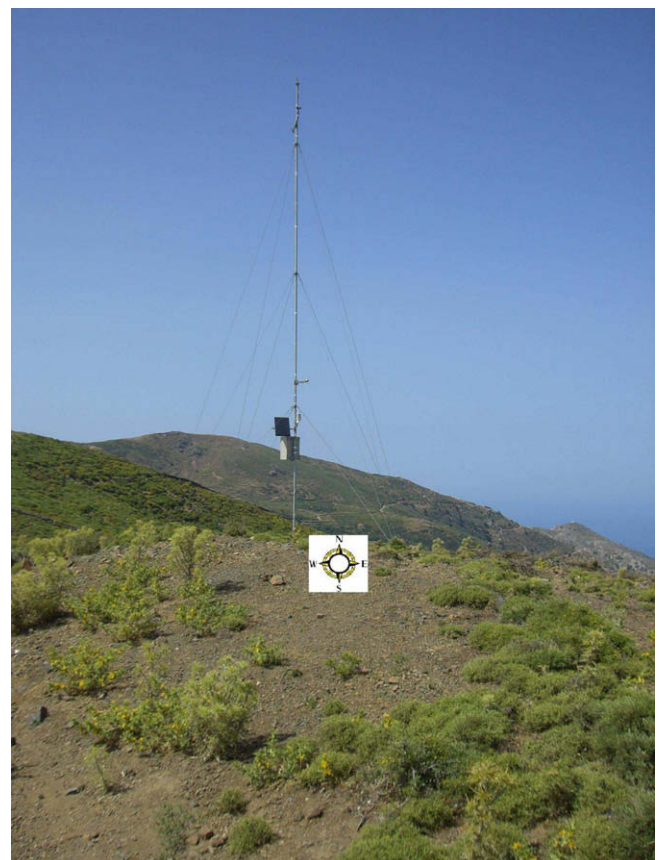


Fig. 2. The wind data measurement mast.

¹ For interpretation of color in Fig. 1, the reader is referred to the web version of this article.

2.3. Wind power density and air density

The estimation of the wind power density is an important factor when assessing the wind potential of a location, as it indicates how much energy per unit of time and swept area of the blades is available at the selected area for conversion to electricity by a wind turbine.

The wind power density is proportional to the density of the air and to the cube of the wind speed. However, air density is a function of temperature T and pressure p , both of which vary with altitude above sea z . Therefore, whenever calculation regarding the wind potential at certain altitude z is performed, the corresponding air density ρ could be evaluated, using the following equation:

$$\rho = \rho_0 \frac{T_0}{T} \left(1 - \frac{\Gamma Z}{T_0}\right)^{\frac{g}{R T_0}} \quad (1)$$

where $g = 9.81 \text{ m/s}^2$ is the gravitational acceleration, $R = 287 \text{ J deg}^{-1} \text{ kg}^{-1}$ is the gas constant, T is the temperature in Kelvin [K], $T_0 = 288 \text{ K}$ ($=273 + 15$), $\rho_0 = 1.225 \text{ kg/m}^3$ is the standard sea-level air density and Γ is the vertical temperature gradient usually taken as: 6.5 K/km .

In the current study, the air density was calculated from the measured temperature, using Eq. (1).

2.4. Weibull distribution of wind speed

A critical factor in wind resource assessment is the distribution of wind speed. The wind speed data obtained, with various observation methods, has usually wide ranges. Therefore, it is necessary to have only a few key parameters that can explain the behaviour of the wide range of wind speed data. In order to minimise the required time and expenses for processing long-term, usually hourly, wind speed data, it is preferred to describe the wind speed variations using statistical functions. There are several probability functions, which can be used to identify suitable statistical distributions for representing wind speed frequency curve. The Weibull and Rayleigh probability density functions are commonly used and widely adopted, with an acceptable accuracy level by numerous wind power studies for different locations worldwide. [13–20].

In Weibull distribution, the variation in wind velocity is characterised by two parameter functions, the probability density function and the cumulative distribution.

The probability density function $f_W(V)$ indicates the probability for which the wind is at a given velocity V . It is given by the following equation:

$$f_W(V) = \frac{k}{c} \cdot \left(\frac{V}{c}\right)^{k-1} \cdot e^{-(V/c)^k} \quad (2)$$

where k is the dimensionless shape parameter showing how peaked the wind distribution is, and c is the dimensionless scale parameter showing how 'windy' the wind location under consideration is.

On the other hand, the cumulative distribution function of the velocity V gives the probability that the wind velocity is equal or lower than V . Therefore, the cumulative distribution $F_W(V)$ is the integral of the probability density function. Hence,

$$F_W(V) = 1 - e^{-(V/c)^k} \quad (3)$$

For the analysis of a wind regime using the Weibull distribution, the Weibull parameters k and c must be calculated. Some of the methods used for determining k and c are:

1. Weibull probability plotting paper method.
2. Standard deviation method.
3. Moment method.

4. Maximum likelihood method.
5. Energy pattern factor method.

Even though all of them are widely used, in the current study the Weibull probability plotting paper method for evaluating the raw data has been used.

In this method, the cumulative distribution function is transformed into a linear form, adopting logarithmic scales. By solving Eq. (3) in terms of e , and taking the logarithm twice, it follows that:

$$\ln\{-\ln[1 - F_W(V)]\} = k \ln(V) - k \ln c \quad (4)$$

The plot of $\ln(V)$ along X axis and $\ln\{-\ln[1 - F_W(V)]\}$ along Y , gives a nearly straight line, the gradient of which is k , whereas $-k \ln c$ represents the intercept. The actual values of k and c can be found by generating the regression equation for the plotted line using any statistical package or a simple spreadsheet. It has been found that for most wind conditions the k values range from 1.5 to 3.0, whereas c ranges between 3 and 8 [6].

The reliability of Weibull distribution in wind regime analysis depends on the accuracy in estimating k and c . For the precise calculation of k and c , the data acquisition over short time intervals is essential. However, in many cases, such information may not be readily available. The existing data may be in the form of the mean wind velocity over a broader time period (e.g. day, month or year). Under such situations, a simplified case of the Weibull model can be derived, by taking $k = 2$. The resulting distribution is known as the Rayleigh distribution.

2.5. Evaluation of Weibull and Rayleigh distributions

In order to be able to evaluate the performance of the considered distributions, the mean root-square error (RMSE) parameter, the chi-square (χ^2) test and the modelling efficiency (EF) can be used.

The RMSE parameter gives the deviation between the predicted and the experimental values, it should be as close to zero as possible, and it is expressed as:

$$\text{RMSE} = \sqrt{\frac{\sum_{i=1}^N (y_i - x_i)^2}{N}} \quad (5)$$

Chi-square test returns the mean square of the deviations between the experimental and the calculated values for the distributions and it is expressed as:

$$\chi^2 = \frac{\sum_{i=1}^N (y_i - x_i)^2}{N - n} \quad (6)$$

As far as, the EF is concerned it shows the ability of the model, and the highest value it can get is 1. EF is calculated as:

$$\text{EF} = \frac{\sum_{i=1}^N (y_i - z)^2 - \sum_{i=1}^N (x_i - y_i)^2}{\sum_{i=1}^N (y_i - z)^2} \quad (7)$$

For both RMSE and chi-square, y_i are the actual values of y , and x_i are the values computed from the correlation equation for the same value of x . The smaller the values of these two parameters are, the better the curve fits. Ideally, both RMSE and chi-square should return zero values.

Finally, for the EF, y_i is the i th experimental data, z is the mean value of the experimental data, x_i is the i th predicted data with the Weibull or Rayleigh distribution, N is the number of observations and n is the number of constants [21,22].

2.6. Wind data collection and evaluation

Data collection was performed for a period of 12 months. The rate of the data recording was 144 per day in 10 min time intervals.

The collected data include date and timestamp, minimum, maximum, average and deviation values of wind speeds at 10 m height, wind directions divided in 16 equally spaced sectors (within 360°), ambient temperature, and relative humidity. Once the required data was stored in the data logger, it was sent directly via a GSM method to the Renewable Energy Laboratory in Athens where it was converted to a spreadsheet for easier processing. Before performing any analysis of the recording, it was necessary to evaluate the percentage of missing data that could have been lost due to weather or the malfunctioning of the instrumentation. It has been found that in overall the missing data did not exceed 7%, a percentage well within the acceptable standards [23]. The distribution of missing data during the year is shown in the Table 1. As can be seen from this table, the missing data are almost equally distributed around the year, except for January where maintenance took place in system.

After establishing this, the analysis and the evaluation of the recordings was performed and the monthly results are presented in the form of tables, pie-charts, histograms and polar diagrams. The corresponding Weibull and Rayleigh distributions were also determined. Additionally, the monthly wind speed variation was obtained in order to check the validity of the data and to extract any useful information regarding the wind potential of the location

Table 1
Monthly distribution of the missing data.

Month	Missing data (%)
August 2006	0.3
September	0.2
October	0.2
November	0.2
December	0.3
January 2007	4.0
February	0.5
March	0.3
April	0.2
May	0.3
June	0.2
July	0.3

under consideration. Finally, the graphical representation of the mean monthly and maximum wind speed was obtained with the corresponding 95% confidence interval.

3. Results and discussion

3.1. Mean wind speed and wind direction analysis

The determination of the wind potential of the selected site was made by analysing in detail the wind characteristics, such as the wind speed, the prevailing direction, their duration and availability, as well as, the resulting power density. Figs. 3 and 4 show the results of the wind speed data analysis. In Fig. 3, the mean monthly and maximum wind speed, with the corresponding 95% confidence interval are presented. The line segments represent the confidence intervals which are twice the standard deviation.

As it can be seen, the windiest months were March and July with the mean wind speed reaching approximately 9 m/s, while the calmest month was June where the mean wind speed did not exceed 6 m/s. Using the data of this diagram, it has been calculated that the corresponding annual mean speed was approximately 7.4 m/s, indicating that the installation of a utility scale power plant would be viable, at least as far as the engineering part is concerned. By checking the pattern of the wind speed distribution, it becomes apparent that the high values recorded from January to March were followed by a significant decrease in April–June. It is believed that these high values were the result of the Vardar, a north wind blowing across the whole of the Balkan Peninsula, especially during the winter. Another factor contributing in this phenomenon was the decrease in temperature during winter and spring. Even though this decrease was expected, it caused thermal convection which in turn resulted in some of the momentum of the upper air (i.e. air that moves at higher velocity) to be transmitted to the surface layers and therefore the noticed increase in the previously mentioned monthly mean wind speeds was caused. On the other hand, the sudden increase observed in July could be attributed to the Etesians, a local circulation system of strong winds affecting the Aegean Sea during the summer months. These observations agreed with the findings of [4,5]. However, a discrepancy,

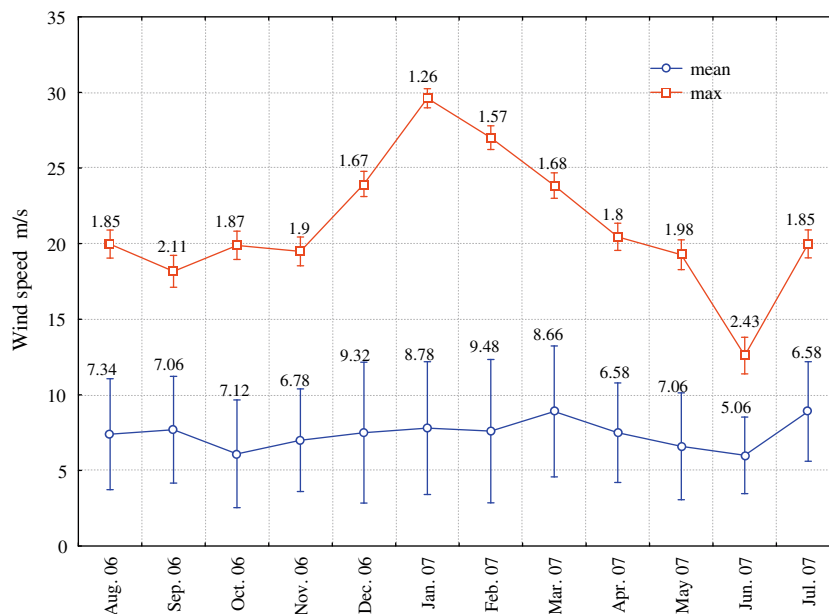


Fig. 3. Mean monthly and maximum wind speed, with the corresponding 95% confidence interval. The line segments represent the confidence intervals which are twice the standard deviation.

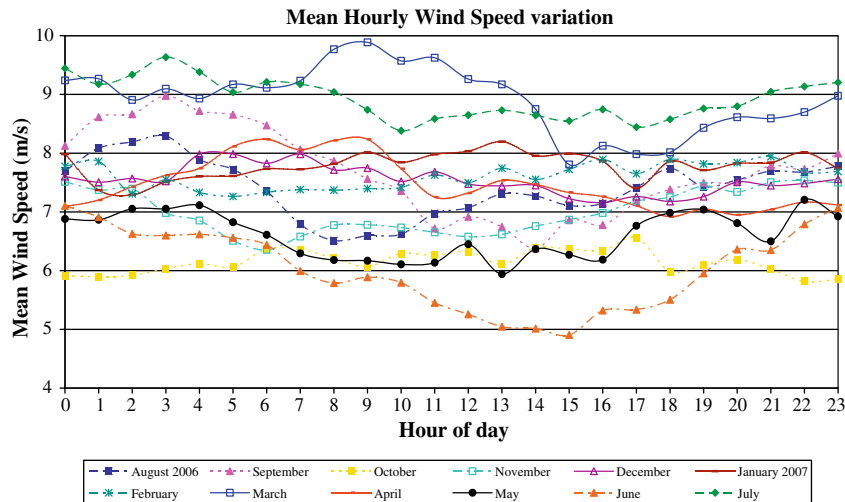


Fig. 4. Diurnal mean wind speeds variation for every month.

in the range of 10%, between their results and those obtained in the current study was observed, which is believed that it was due to the different altitude of the measurement mast and the number of daily observations.

When observing the monthly variation of the mean wind speed with respect to the corresponding maximum value, as shown in Fig. 3, it is apparent that the biggest difference occurred in January.

It is believed that this difference was due to turbulence and mountain winds phenomena, both of which could be responsible for the occasionally high values in the wind speed. Also, from the Fig. 3 it can be seen that the mean wind speeds are characterised by higher values of standard deviation with respect to those of the maximum wind speeds as is normal to expect.

Another interesting outcome of the analysis of the mean wind speed was its diurnal variation. As shown in Fig. 4, the diurnal variation can be taken as approximately constant for all the months considered, apart from June and September where a significant depression occurred between 10 am and 7 pm, reaching a minimum about at 2 pm, and March during which there was a strong front from 7 am to 2 pm reaching a maximum about at 9 am. It is believed that the observed stability serves well the expected energy demands of Naxos Island, both during the day and night time, and that any excess in available energy could be stored. This figure also shows that during the summer months (i.e. May–September), the wind speed start to decrease slightly in the early morning and restart to increase early afternoon. The diurnal variation is more stable during the winter months (i.e. December–February). This may be explained by the low temperature stratification. An argument that may be used to explain the diurnal variation, for the months March–November, assuming constant horizontal pressure force, is the variation in atmospheric stability, which in turn affects the vertical exchange in momentum. Vertical exchange in momentum which would be most pronounced during early afternoon because of thermal convection, would result in an increase of wind speed. At night the vertical exchange in momentum is less.

It should be mentioned that as the available data corresponded only to 1 year, no conclusive results should be safely drawn, and hence, further investigation should be carried out, since neglecting the diurnal wind patterns could result in significant under- or overestimation of the wind energy potential of the measurement site. As an overall overview though, it is safe to say that the selected location presented a fairly stable and quite high pattern on the diurnal annual wind speed variation.

3.2. Wind direction

Usually, in wind data analysis, the prediction of the wind direction is also very important, especially when planning the installation and the micro-siting of a wind turbine or a wind farm. The annual wind rose based on time, are shown in Fig. 5.

Most of the time the prevailing winds in Naxos Island were the north–northeastern, the northeastern, and the west–southwestern. This was a well-expected outcome since this particular region is influenced by the winds blowing from the Balkan Peninsula. Therefore, it is worthwhile to remark that the area under investigation showed a significant stability as far as the percentage of time a wind was blowing from a particular direction was concerned.

Nearly similar trends can also be seen in Fig. 6, where the annual wind rose based on energy, are presented.

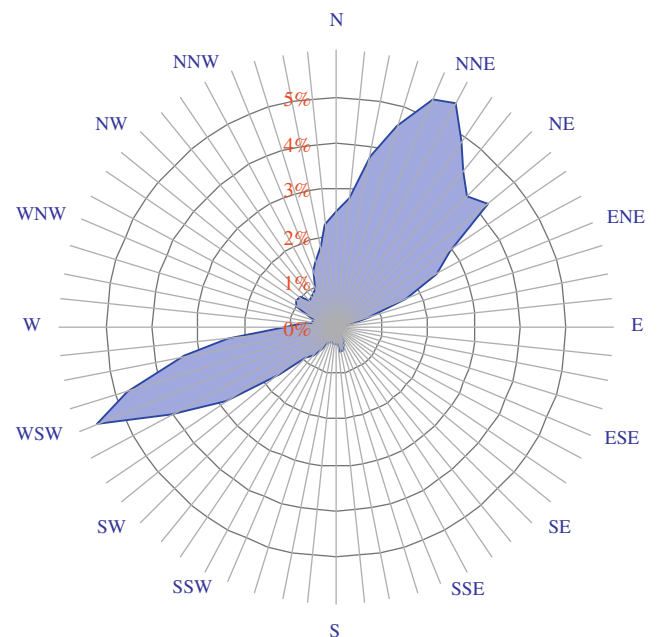


Fig. 5. Annual wind rose based on time.

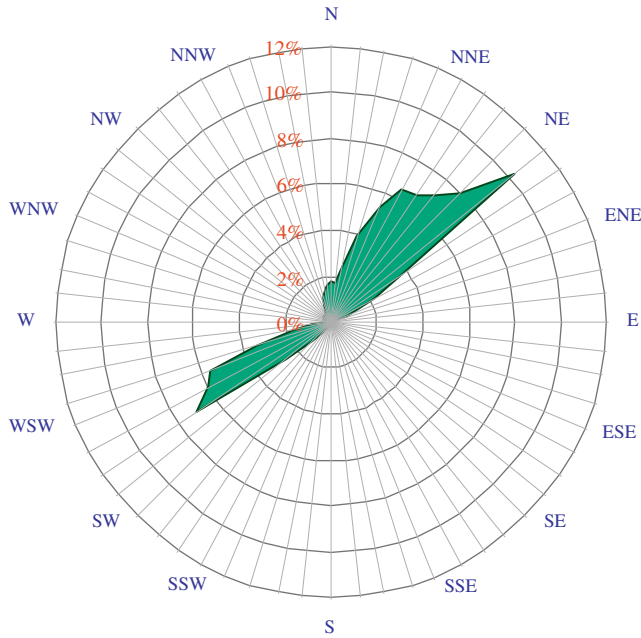


Fig. 6. Annual wind rose based on energy.

Again the prevailing directions indicated were the northeastern, the north–northeastern, and the west–southwestern. It should be mentioned that the percentage of energy depicted in the wind roses of Fig. 6 corresponds to the distribution of the available wind energy and not that delivered by a potentially installed wind turbine. Although, the difference is relatively small, it is mainly associated with the cases where the wind speed from a particular direction is larger than the turbine’s cut-out speed.

Finally, in both Figs. 5 and 6, the calms have not been considered as it is believed that during the calms the direction recorded by the wind vanes was not necessarily representative. The percentage of calm conditions, where the wind speed is less than or equal to 2 m/s, is shown in Table 2. It is apparent from this table that the high percentage of calm conditions is found in May, October and December.

Conclusively, the outcomes of the analysis of the wind direction are presented in Figs. 7 and 8, in which the prevailing wind directions and the corresponding percentages of time and available wind energy for each month studied are included.

When comparing these figures, it becomes obvious that the best wind sector based on time did not necessarily coincide with the best sector based on the available wind energy.

This remark was not unexpected when considering that although wind might be blowing from one direction for a relatively long period, the corresponding speeds recorded might not be high

Table 2
Monthly distribution of the calm conditions.

Month	Number of calms%
August 2006	5.3
September	4.0
October	11.3
November	5.2
December	9.6
January 2007	3.2
February	6.0
March	2.8
April	3.4
May	9.1
June	6.1
July	1.2

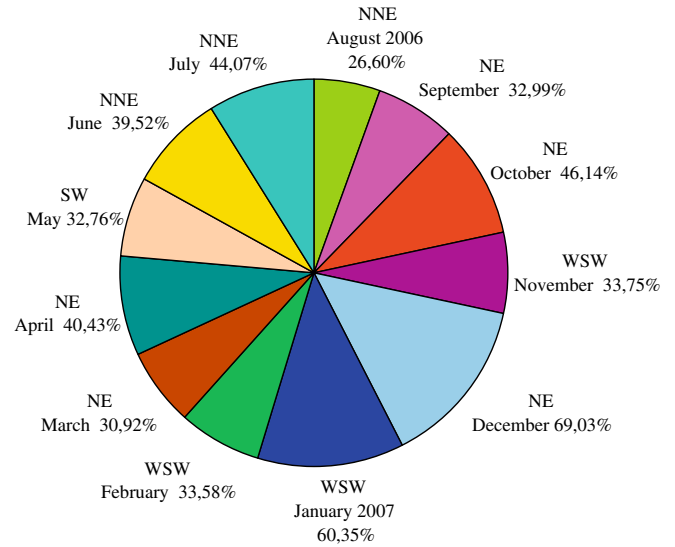


Fig. 7. Best monthly prevailing wind directions based on available wind energy.

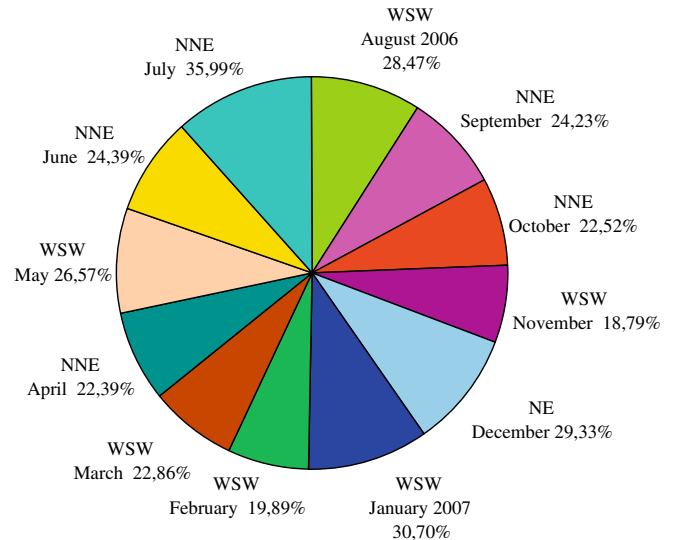


Fig. 8. Best monthly prevailing wind directions based on time.

enough to produce the maximum available energy. Therefore, only in November, December, January, February, June and July the best wind sector based on time was the same as the corresponding best sector based on energy. The highest percentage of time wind was blowing from a particular direction, namely the north–northeastern, was 35.99%, and it was recorded in July. On the contrary, the highest percentage of available wind energy was obtained from the northeastern direction, it was 69.03%, and it was recorded in December.

3.3. Wind power density analysis

The results of the wind speed variation and the prevailing wind directions which characterised the location under investigation were further analysed with respect to the corresponding mean wind power density. Fig. 9 shows a histogram of the monthly variation of the mean wind power density.

As it can be seen, in October and in November the estimated mean wind power densities were almost half of that obtained in

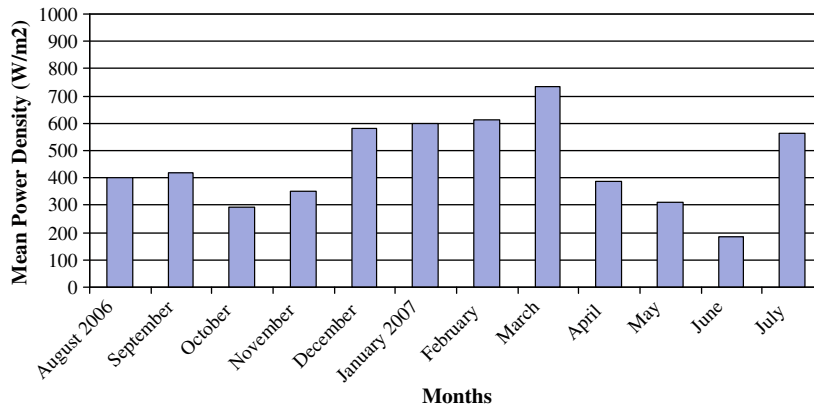


Fig. 9. Monthly variation of the mean power density.

March (i.e. maximum value). Moreover, a gradual increase was observed during the winter months (i.e. December–February), with a peak value of approximately 730 W/m^2 in March. This increase was followed by a sudden decrease from the end of spring to the beginning of summer (i.e. April–June), and an increase again in July. The observed increase in July was attributed to the Etesian winds, which, as already explained, characterised this particular period. As already mentioned, the highest value was around 730 W/m^2 in March, while the lowest value was approximately 180 W/m^2 in June. The resulting mean annual wind power density was estimated to be 420 W/m^2 . This value, and the corresponding annual mean wind speed, verifies that the northeastern part of Naxos Island falls into Class 7 of the commercially international system of wind classification according to [24].

A comparison of the monthly mean wind speeds and mean wind power density is shown in Fig. 10. It is clear that the two curves have similar changing trend. However, the rate of change is different as a small variation in the wind speed can cause larger wind power density predictions due to the fact that the wind power density is proportional to the cube of the wind speed. This effect is more pronounced at higher wind speed conditions.

To conclude with, from the analysis of the collected data, it became apparent that for the purpose of mapping the variation of the wind potential of the northeastern part of Naxos Island, it was bet-

ter to choose the wind power density since it incorporated not only the distribution of wind speeds, but also the dependence of the power density on air density and on the cube of the wind speed.

3.4. Probability density functions

Simple knowledge of the mean wind speed of the selected area could not be taken as sufficient for obtaining a clear view of the available wind potential. Therefore, in order to surpass the non-predictability of the wind characteristics, a statistical analysis was considered necessary. For this reason, Weibull and Rayleigh distribution models were applied.

Fig. 11 shows the probability density function of the annual wind speed distribution, in which Weibull and Rayleigh models have been fitted.

The probability density function indicates the fraction of time for which a wind speed possibly prevails at the area under investigation. Hence, it can be observed in Fig. 11 that the most frequent wind speed expected in the area under investigation is around 7 m/s , a value which corresponds to the peak of the probability density function curve. This result agrees with that already obtained from the initial analysis of the mean wind speed. It is also clear in Fig. 11 that the chances of wind speed exceeding 20 m/s in this region were very limited.

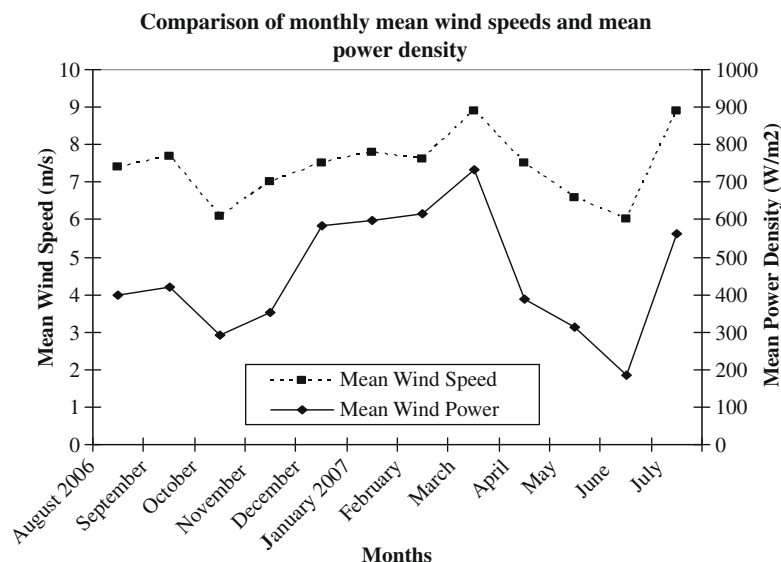


Fig. 10. Comparison of the monthly mean wind speeds and mean wind power density.

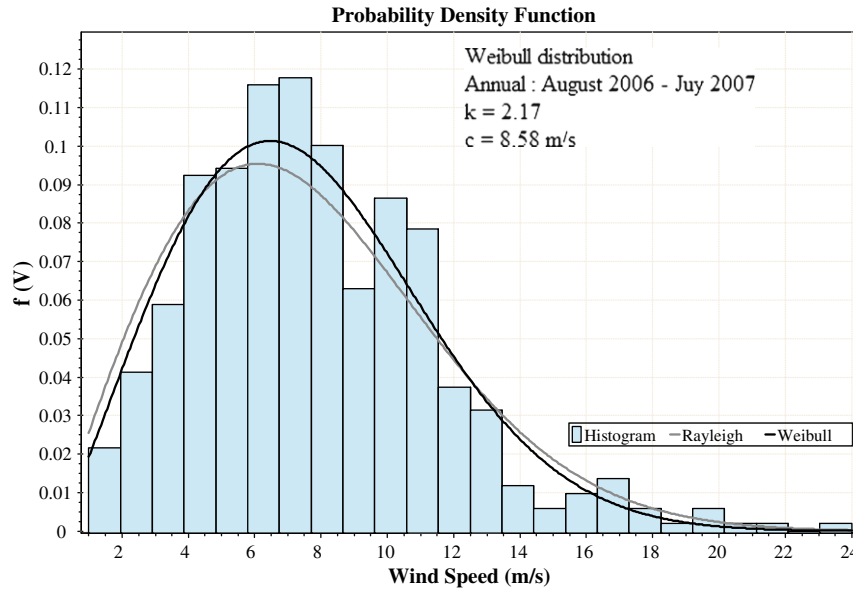


Fig. 11. Probability density distribution of annual wind speeds.

The previously mentioned remarks were further supported by the Weibull curve. On the contrary, Rayleigh curve was slightly shifted to the left, indicating a lower possibility of a lower maximum wind speed occurring. The relatively large annual values of the Weibull parameters k and c found, 2.17 and 8.58 m/s, respectively, verified the existence of a high wind potential of good quality in the area. Both parameters will be further analysed later in this section.

Another important aspect considered during the statistical analysis was the prediction of the time for which a potentially installed, in this area, wind turbine could be functional. In order to achieve that, the determination of the cumulative distribution function was required. Since this function indicates the fraction of time the wind speed is below a particular speed, by taking the difference of its values the corresponding time for which the turbine would be functional can be estimated.

The obtained cumulative function is shown in Fig. 12. Weibull and Rayleigh models have also been included.

Even though the difference between the two models was relatively small, Weibull appeared to represent the actual data better.

In order to evaluate the performance of the two models considered, an error analysis was carried out. The mean root-square error (RMSE) parameter, the Chi-square (χ^2) test, and the modelling efficiency (EF) test were used in the current investigation, and the results are presented in Table 3.

According to these tests, a distribution function better approximates the actual data when the values of RMSE and χ^2 are close to zero, and the values of EF approach unity. By checking the results presented in Table 3 it is clear that Weibull model described better the observed data.

These results were also in accordance with the probability difference of the two models shown in Fig. 13.

After establishing the performance of the two distribution functions, the Weibull parameters k and c were further studied. Figs. 14 and 15 present the annual variation of k and c parameters, respectively.

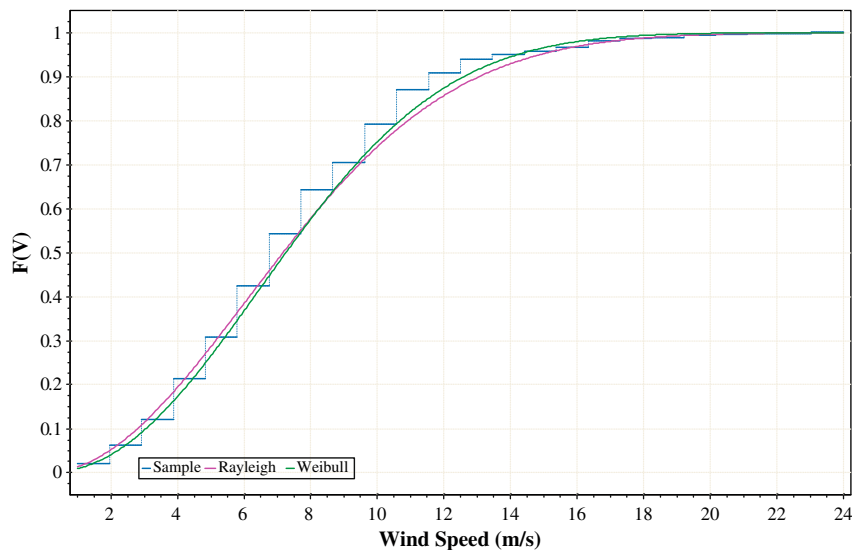
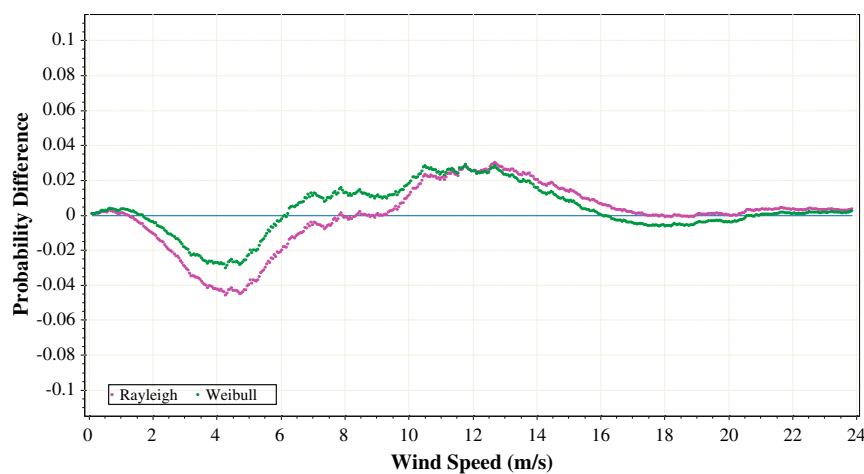
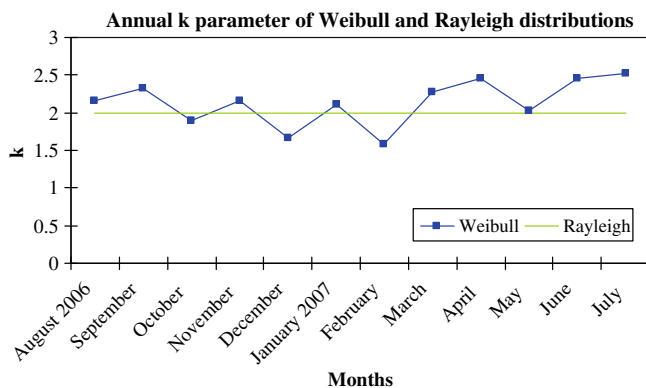
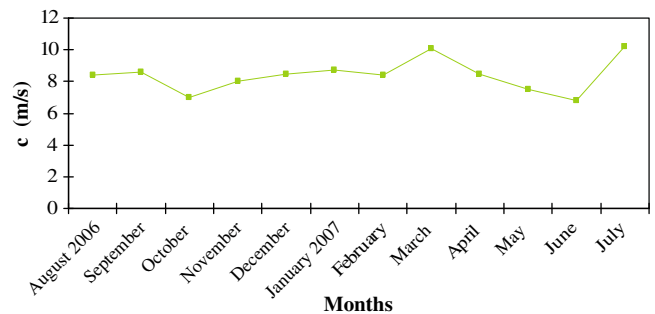


Fig. 12. Cumulative distribution function of the annual mean wind speed.

Table 3

Error analysis of the statistical models used.

	Weibull			Rayleigh		
	RMSE	χ^2	EF	RMSE	χ^2	EF
August 2006	6.512×10^{-3}	4.665×10^{-5}	0.971	6.786×10^{-3}	4.824×10^{-5}	0.968
September	10.096×10^{-3}	11.4×10^{-5}	0.925	10.634×10^{-3}	13.82×10^{-5}	0.904
October	8.786×10^{-3}	8.390×10^{-5}	0.957	8.023×10^{-3}	6.706×10^{-5}	0.964
November	10.057×10^{-3}	11.2×10^{-5}	0.946	11.685×10^{-3}	14.4×10^{-5}	0.927
December	12.8×10^{-3}	17.9×10^{-5}	0.853	15.575×10^{-3}	25.3×10^{-5}	0.783
January 2007	12.056×10^{-3}	15.8×10^{-5}	0.916	13.381×10^{-3}	18.7×10^{-5}	0.896
February	8.393×10^{-3}	7.66×10^{-5}	0.941	12.871×10^{-3}	17.3×10^{-5}	0.862
March	7.118×10^{-3}	5.527×10^{-5}	0.955	8.27×10^{-3}	7.153×10^{-5}	0.939
April	11.126×10^{-3}	13.6×10^{-5}	0.936	15.336×10^{-3}	24.6×10^{-5}	0.881
May	4.02×10^{-3}	1.779×10^{-5}	0.989	5.37×10^{-3}	3.036×10^{-5}	0.980
June	10.503×10^{-3}	13.1×10^{-5}	0.951	18.452×10^{-3}	36.9×10^{-5}	0.851
July	15.299×10^{-3}	25.7×10^{-5}	0.897	27.6×10^{-3}	79.8×10^{-5}	0.666
Annual	9.730×10^{-3}	11.388×10^{-5}	0.936	12.867×10^{-3}	21.044×10^{-5}	0.880

**Fig. 13.** Probability difference of Weibull and Rayleigh models.**Fig. 14.** Annual variation of Weibull shape parameter k .**Fig. 15.** Annual variation of Weibull scale parameter c .

It can be noted that the values of k varied significantly during the year with the minimum value being slightly over 1.5 in February and the maximum value being close to 2.5 in July. On the other hand, the scale parameter c had a smaller variation than k parameter, and it ranged from approximately 7 m/s in October to 10 m/s in March and July. These results were higher than the findings of Katsoulis [4] who estimated k to be 1.4 and c 6.9 m/s. This can be easily understood when considering that the wind potential of the region cannot be taken as high but unaltered. Moreover, the peaked wind distribution observed can be correlated with the high values of k parameter.

4. Conclusions

The main conclusions drawn from this investigation into the wind characteristics of the northeastern part of Naxos Island were:

- The Central Aegean Sea shows a very pronounced wind potential.
- The windiest months were March and July with the mean wind speed reaching approximately 9 m/s, while the calmest month was June where the mean wind speed did not exceed 6 m/s.
- The annual mean wind speed was approximately 7.4 m/s.
- Occasionally high values in the wind speed were due to turbulence and mountain winds phenomena.

- The selected location presented a fairly stable and quite high pattern on the diurnal annual wind speed variation.
- The measurement site falls under Class 7, indicating that it was suitable for large scale electricity generation.
- Most of the time the prevailing winds in the area under investigation were the northeastern, the north–northeastern, and the west–southwestern.
- The highest value of the mean power density was around 730 W/m^2 in March, while the lowest value was approximately 180 W/m^2 in June.
- The mean annual wind power density was estimated to be 420 W/m^2 .
- The large annual wind power density observed in the area was the result of the winter months contributions.
- The high speed values could be attributed to Vardar wind blowing across the Balkan Peninsula during the winter and the Etesians affecting the Aegean Sea during the summer months.
- Weibull parameters k and c were found to be 2.17 and 8.58 m/s, respectively.
- Weibull distribution represented the actual data better than the Rayleigh distribution.

References

- [1] Mariopoulos EG, Karapiperis LN. Aeolian energy and its use in Greece. *Tech Chron* 1953;345–346:1–15.
- [2] Galanis N. The production of electricity from the wind: a preliminary feasibility study for Greece. *J Wind Eng* 1977;1:241–9.
- [3] Tselepidaki H, Theoharatos G, Lalas DP. Means for the determination of wind energy potential in Greece. In: *Proceedings of cong. Wind energy and industrial aerodynamics*, November 1980, Athens, Greece.
- [4] Lalas DP, Tselepidaki H, Theoharatos G. An analysis of wind potential in Greece. *J Solar Energy* 1983;30(6):497–505.
- [5] Katsoulis BD. A survey on the assessment of wind energy potential in Greece. *J Theor Appl Climatol* 1993;47:51–63.
- [6] Kaldellis JK. *Wind energy management*. Athens: Stamoulis Publications; 1999.
- [7] Kaldellis JK, Kavadias KA. *Experimental applications in renewable energy sources*. Athens: Stamoulis Publications; 2001.
- [8] Kaldellis JK. Optimum autonomous wind-power system sizing for remote consumers, using long-term wind speed data. *J Appl Energy* 2002;71:215–33.
- [9] Ozerdem B, Turkeli M. An investigation of wind characteristics on the campus of Izmir Institute of Technology. *J Renew Energy* 2003;28:1013–27.
- [10] Akpinar E Kavak. A statistical investigation of wind energy potential. *Energy Sourc, Part A: Recov Utilization Environ Effects* 2006;28(9):807–20.
- [11] Gökçek M, Bayülken A, Bekdemir Ş. Investigation of wind characteristics and wind energy potential in Kirklareli, Turkey. *J Renew Energy* 2007;32:1739–52.
- [12] Ucar A, Balo F. Investigation of wind characteristics and assessment of wind-generation potentiality in Uludağ-Bursa, Turkey. *J Appl Energy* 2009;86:333–9.
- [13] Celik AN. A statistical analysis of wind power density based on the Weibull and Rayleigh models at the southern region of Turkey. *Renew Energy* 2003;29:593–604.
- [14] Garcia A, Torres JL, Prieto E, De Francisco A. Fitting probability density distributions: a case study. *Sol Energy* 1998;62(2):139–44.
- [15] Hennessey JP. Some aspects of wind power statistics. *J Appl Meteorol* 1977;16:119–28.
- [16] Jamil M, Parsa S, Majidi M. Wind power statistics and an evaluation of wind energy density. *Renew Energy* 1995;6:623–8.
- [17] Justus CG, Hargraves WR, Mikhail A, Graber D. Methods of estimating wind speed frequency distributions. *J Appl Meteorol* 1978;17:350–3.
- [18] Kose R, Ozgur MA, Erbas O, Tugcu A. The analysis of wind data and energy potential in Kutahya, Turkey. *Renew Sustain Energy Rev* 2004;8:277–88.
- [19] Rehman S. Wind energy resources assessment for Yanbo, Saudi Arabia. *Energy Convers Manage* 2004;45:2019–32.
- [20] Vogiatzis N, Kotti K, Spanomitsios S, Stoukides M. Analysis of wind potential and characteristics in North Aegean, Greece. *Renew Energy* 2004;29:1193–208.
- [21] Li M, Li X. Investigation of wind characteristics and assessment of wind energy potential for Waterloo region, Canada. *J Energy Convers Manage* 2005;46:3014–33.
- [22] Chang TJ, Wu YT, Hsu HY, Chu CR, Liao CM. Assessment of wind characteristics and wind turbine characteristics in Taiwan. *J Renew Energy* 2003;28:851–71.
- [23] AWS Scientific Inc. *Wind resource assessment handbook*. National Renewable Energy Laboratory; 1997.
- [24] Elliott DL, Schwartz MN. *Wind energy potential in the United States*, PNL-SA-23109. Richland, WA: Pacific Northwest Laboratory; September 1993 [NTIS no. DE94001667].